

Menthol-Activated Cells in the Reward-Addiction Neurocircuitry

Ozra Dehkordi^{1,2*}, Richard M Millis³, Maryam M Dalivand¹, Melanie Swang², Martha I Dávila-García⁴

¹Department of Neurology, Howard University Hospital Washington D.C. 20060, United States

²Department of Physiology & Biophysics, Howard University College of Medicine Washington, D.C. 20059, United States

³Department of Pathophysiology, American University of Antigua College of Medicine, Antigua & Barbuda, West Indies

⁴Department of Pharmacology, Howard University College of Medicine Washington, D.C. 20059, United States

ABSTRACT

Background: Menthol, a commonly used flavoring additive in cigarettes has been found to facilitate smoking initiation and nicotine addiction. However, the neuroanatomical and neurochemical targets of menthol within the reward-addiction neurocircuitry remain unknown. In the present study in mice, we hypothesized that dopaminergic and GABAergic neurons of the reward-addiction circuitry are among the initial targets of menthol in the CNS.

Methods: We tested this hypothesis by utilizing c-Fos immunohistochemical techniques and double labeling to identify the anatomical location of menthol activated cells with respect to tyrosine hydroxylase (TH) immunoreactive (IR) dopaminergic and GAD67-GFP positive GABAergic cells.

Results: Menthol (100 mg/kg, IP) produced c-Fos activation at multiple sites of the mesocorticolimbic reward-addiction pathways including several structures previously shown to be activated by nicotine such as the periaqueductal gray (PAG), dorsal raphe (DR), ventral tegmental area (VTA), several thalamic and hypothalamic nuclei, amygdala, nucleus accumbens (NAcc) insular cortex, piriform cortex, anterior olfactory nucleus and cingulate-orbitofrontal cortex. Double-labeling studies showed that neither dopaminergic nor GABAergic neurons in VTA showed menthol-induced c-Fos immunoreactivity. Dopaminergic cells in PAG/DR region and hypothalamus were also devoid of menthol-induced c-Fos immunoreactivity. In addition to VTA, the GABAergic cells of NAcc and cingulate-orbitofrontal cortex were not targeted by menthol.

Conclusion: The present study identifies several sites, including those of the mesocorticolimbic reward-addiction pathways that contain neurons activated by IP administration of menthol. However, neither dopaminergic nor GABAergic neurons appear to be the initial targets of menthol in the reward-addiction neurocircuitry.

Keywords: Menthol; GABAergic neurons; Dopaminergic neurons; Nicotine addiction

INTRODUCTION

One of the sensory perceptions associated with cigarette smoking that has received much attention is the cooling sensation induced by menthol, a commonly used flavoring additive in cigarettes and e-cigarettes [1-3]. Several studies have suggested that menthol facilitates smoking initiation and nicotine addiction [4-6]. However, little is still known about the anatomical and molecular components within the reward-addiction pathways that make it so difficult for smokers, particularly smokers of mentholated cigarettes, to quit, why they have a higher relapse rate, and why it may be easier for naïve individuals to get “hooked” faster when they begin smoking mentholated cigarettes [7-11]. This issue is of particular significance for the African American population of

which more than 80% smoke mentholated cigarettes [12-14].

Much work has been done to study how menthol affects gene expression and functional changes of nicotinic receptors in the reward-addiction neurocircuitry [15-19]. However, little is known about the neurochemical profile of CNS neurons that are the direct targets of menthol. In the present study, we used c-Fos immunohistochemical techniques to identify cells within the reward-addiction pathways that are activated by IP administration of menthol. We then determined whether dopaminergic and/or GABAergic cells are the initial targets of menthol in the ventral tegmental area (VTA), periaqueductal gray (PAG), dorsal raphe (DR), nucleus accumbens (NAcc), cingulate cortex and other reward-related areas.

*Correspondence to: Ozra Dehkordi, Associate Professor, Department of Neurology, Howard University Hospital Washington, D.C. 20060, United States, Tel: +1 202 865 1978; Fax: +1 202 865 1977, Email: odehykordi@howard.edu

Received: July 29, 2019; Accepted: August 07, 2020; Published: August 14, 2020

Citation: Dehkordi O, Millis RM, Dalivand MD, Swang M, Dávila-García MI. (2020) Menthol-Activated Cells in the Reward-Addiction Neurocircuitry. J Alcohol Drug Depend 8: 332. doi: 10.35248/2329-6488.20.8.332.

Copyright: ©2020 Ozra Dehkordi, et al. This is an open-access article distributed under the terms of the Creative Commons Attribution License, which permits unrestricted use, distribution, and reproduction in any medium, provided the original author and source are credited.

MATERIALS AND METHODS

Animals: All experiments were performed in male and female CD-1 mice and/or GAD67-GFP knock-in mice (2-3-months-old) weighing 20-25 g. The age of the animals was within the broadly defined age range of adolescence, a time at which animals are known to be more vulnerable to the effects of nicotine. All procedures including the anesthesia and surgery were reviewed and approved by the Institutional Animal Care and Use Committee (IACUC) of Howard University. All efforts were made to minimize the number of animals used and their suffering.

Experimental protocol

Animals (N=15) were housed at room temperature (22-24°C) with water and food being freely available. To reduce the nonspecific effects of handling and experimental environment, animals were handled daily and exposed to the same conditions as during the actual experiments. Following an adaptation period of 3-4 days, the mice received an IP injection of vehicle (6% ethyl alcohol, v/v) and/or DL-menthol (100 mg/kg, IP; Sigma Aldrich, St. Louis, MO). Previous studies have used various routes of administration and a wide range of concentrations to evaluate the acute pharmacological effects of menthol in experimental animals [16,20-22]. The dose of menthol (100 mg/kg, IP) selected for the present study was based on previous studies in mice evaluating the acute effects of (-)-menthol on nicotine pharmacokinetics [16]. This dose of menthol was shown to cause a significant decrease in the clearance of nicotine and increase in its AUC compared to a control vehicle [16]. This dose was also reported to enhance nicotine-induced antinociception and hypothermia [16]. In addition, repeated administration of this dose of menthol to nicotine-exposed mice was reported to significantly enhance the intensity of nicotine's physical and affective withdrawal signs [16]. Menthol was injected in volumes of 0.2 ml/injection. Two hours after IP injection of vehicle and/or menthol, the mice were anesthetized with 5% isoflurane and perfused transcardially with saline, followed by 4% paraformaldehyde in 0.1 M phosphate buffer (PB) at pH 7.4. After perfusion, the brains were post-fixed in 4% paraformaldehyde for 1 h and then cryoprotected in a 30% sucrose solution for a minimum of 2 days. Coronal sections of the brains were cut at 40 µm using a Bright OTF Cryostat (Hacker Instruments and Industries) and stored in 0.5% sodium azide in 0.1 M PB (pH 7.4).

Immunohistochemistry: Immunohistochemical procedures were performed using free floating sections as follows: Briefly, 1-in-5 series of brain sections extending from bregma - 7.31 mm to bregma 2.33 mm [23] were rinsed three times in 0.1 M phosphate buffered saline (PBS) at pH 7.4 and processed for immunohistochemical labeling according to the following protocols.

Sequential double labeling of menthol-induced c-Fos activated cells and tyrosine hydroxylase (dopaminergic) immunoreactive cells: These experiments were conducted to identify the menthol-activated cells and to determine if dopaminergic cells of VTA, DR, PAG and/or hypothalamus are the initial targets of acute IP administration of menthol in the CNS (N=5). Nonspecific binding was blocked by incubating the tissues overnight in loading buffer containing 2% normal donkey serum (NDS: Santa Cruz Biotechnology) and 0.3% Triton X-100. Tissues were then washed and incubated with 0.1 M phosphate buffer saline (PBS) cocktail consisting of 0.3% Triton X-100, rabbit anti-c-Fos (Millipore Cat # ABE457, RRID:AB_2631318, 1:1,000) and mouse anti-tyrosine hydroxylase (TH: Sigma-Aldrich Cat# T2928, RRID:AB_477569,

1:1,000) antibodies at 4°C for 24-48 h. The sections were then washed and incubated in Alexa Fluor 594 donkey anti-rabbit secondary antibody (Jackson ImmunoResearch, 1:100) in PBS for 2½ h. After washing in PBS, sections were incubated in PBS containing CY5 donkey anti-mouse secondary antibodies (Jackson ImmunoResearch, 1:100) for 2½ h. Finally, the sections were rinsed in PBS mounted on slides, and cover-slipped using Vecta Shield (Vector Laboratories) anti-fade mounting media.

Sequential double immunohistochemical labeling of menthol-induced c-Fos activated cells and GABAergic cells: These experiments were conducted to determine if GABAergic cells of VTA, NAcc and/or cingulate and orbitofrontal cortex (MO/A25) are the initial targets of acute menthol in the CNS (N=5). GABAergic neurons are usually identified by immunohistochemical labeling of enzymes that are involved in GABA synthesis, namely GAD65 and GAD67 enzymes. Thus, this group of experiments was carried out in GAD67-GFP knock-in mice that co-express Green Fluorescent Protein (GFP) with the native protein GAD67, which allows for these neurons to be easily identified with the use of fluorescent microscopy. These mice, which have been successfully bred in our animal facilities, were generously provided by Dr. Scott Steffensen of Brigham Young University (founder: Yuchio Yanagawa, Gumma University, Japan). Briefly, tissue sections were rinsed in PBS and nonspecific binding was blocked by incubating the tissues overnight in loading buffer containing 2% NDS and 0.3% Triton X-100. Tissues were then washed and incubated with a PBS cocktail consisting of 0.3% Triton X-100 and rabbit anti-c-Fos (Millipore Cat # ABE457, RRID:AB_2631318, 1:1,000) at 4°C for 48 h. After washing in PBS, the sections were incubated in PBS containing Alexa Fluor 594 donkey anti-rabbit secondary antibody (Jackson ImmunoResearch, 1:100) for 2½ h. Sections were then washed with PBS mounted on slides, and cover-slipped using Vecta Shield (Vector Laboratories) anti-fade mounting media.

Data analysis

High-resolution fluorescent images were acquired using a Nikon (Nikon Instruments, Melville, NY) microscope equipped with the adequate filter systems to observe three different fluorescent dyes: Green, red and CY5. Co-localization of c-Fos immunoreactive (IR) cells with TH IR dopaminergic and/or GAD67 GFP-positive GABAergic cells was detected by sequential capturing of the images, alternating between filters appropriate for each labeling and by analyzing the merged images of the exact same sites. Images from all the brain regions of interest were captured at 4x, 10x and 20x magnification and minor adjustments of brightness and contrast were made using Adobe Photoshop CS3.

Cell counting

A semi-quantitative estimate of the total number of menthol or vehicle-induced c-Fos-activated cells in rostral VTA (VTAR), NAcc and MO/A25 was performed. A representative 40-µm section from each of the aforementioned structures was selected from each animal from experimental (N=5) and control groups (N=5). A well-defined area based on anatomical landmarks was chosen for analysis. The c-Fos IR cells were counted in a single plane and overlapping cells were counted if they were distinguishable by a staining intensity greater than that of the background. Statistical analysis was performed using one-way analysis of variance (ANOVA) to compare the effects of vehicle vs. menthol in the aforementioned areas. When effects were shown to be significant, a post hoc t-test was performed for pairwise comparison. The significance level was

set at $P \leq 0.05$. Data are expressed as means \pm standard errors.

RESULTS

Menthol-induced c-Fos-activated cells

Menthol-induced c-Fos activated cells were observed at multiple sites of the CNS, including several structures previously shown to be activated by nicotine [24,25]. In VTA, menthol-induced c-Fos activated cells were seen in areas overlapping retromamillary nucleus (RM), interpeduncular nucleus, rostral (IPR), interfascicular nucleus (IF) and rostral linear nucleus (RLi). Other areas of the reward addiction circuitry activated by menthol included MO/A25 and NAcc (Figure 1). Semi-quantitative analysis of the number of c-Fos IR cells in VTAR, NAcc and MO/A25 demonstrated that the number of menthol-induced c-Fos activated cells was significantly greater for menthol-treated compared to vehicle-treated animals ($P \leq 0.05$). At the VTAR, the number of c-Fos activated cells in the controls was 17.6 ± 12.4 vs. 55.0 ± 15.0 in the menthol-treated animals ($P < 0.05$). At the NAcc and MO/A25, the numbers of c-Fos activated cells in the controls were 11.5 ± 5.0 and 13.3 ± 9.0 vs. 44.5 ± 15.1 and 41.8 ± 6.5 in the menthol-treated animals,

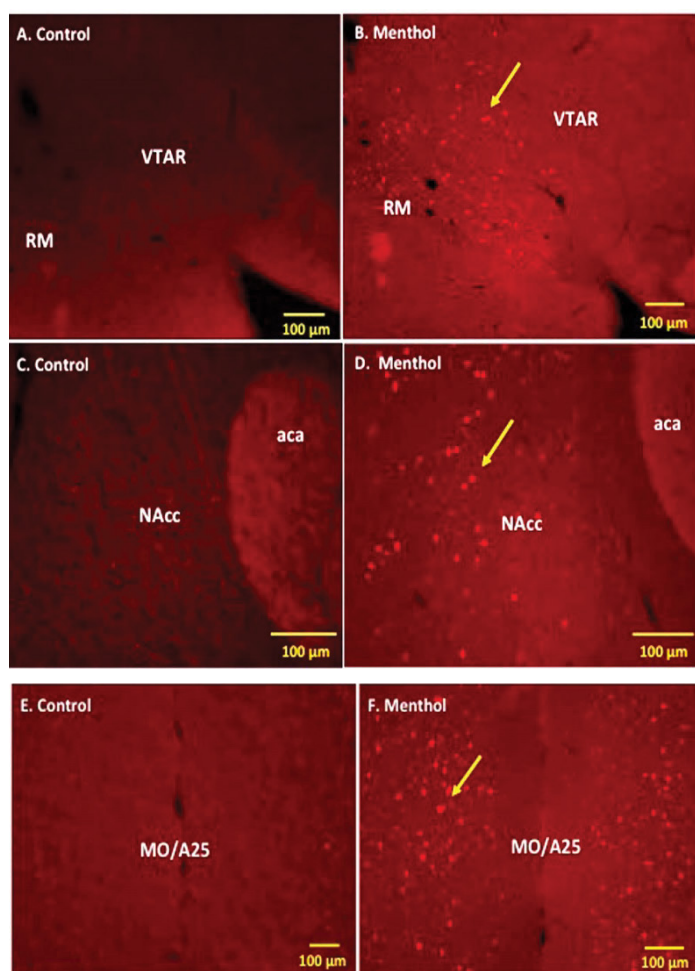


Figure 1: Immunofluorescence staining demonstrating the anatomical location of menthol-induced c-Fos activated cells with respect to the main structures of the nicotine reward-addiction circuitry. Panels A, C and E: Representative control data demonstrating c-Fos immunoreactivity observed in the rostral ventral tegmental area (VTAR), nucleus accumbens (NAcc) and cingulate/medial orbital cortex (MO/A25) following intraperitoneal (IP) injection of vehicle. Panels B, D and F: c-Fos immunoreactive (IR) cells in VTA, NAcc and MO/A25 following IP injection of menthol. Arrows point to representative c-Fos IR neurons. Abbreviations: RM: Retromamillary nucleus; aca: Anterior commissure, anterior part; A25: Cingulate cortex; MO: Medial orbital cortex.

respectively ($P < 0.05$).

Menthol also induced mild to intense c-Fos activation at several other sites in the CNS (Figure 2). In brainstem, mild to moderate menthol activated cells were seen in areas overlapping ventrolateral medulla (VLM), nucleus of solitary tract (NTS), dorsal motor nucleus of vagus, PAG, DR and superior colliculus (SC). In diencephalon, intense c-Fos immunoreactivity was observed mainly in areas overlying paraventricular nucleus of hypothalamus (PVN), posterior hypothalamic area (PH), arcuate hypothalamic nucleus (Arc), ventromedial hypothalamic nucleus (VMH), magnocellular nucleus of lateral hypothalamus (MCLH), paraventricular thalamic nucleus (PVT), medial geniculate nucleus (MGV) and parasubthalamic nucleus (PSTh). Other CNS areas activated by menthol include amygdaloid nucleus, bed nucleus of stria terminalis (BNST) lateral septal nucleus ventral part, angular insular cortex (AIP), piriform cortex (Pir), anterior olfactory

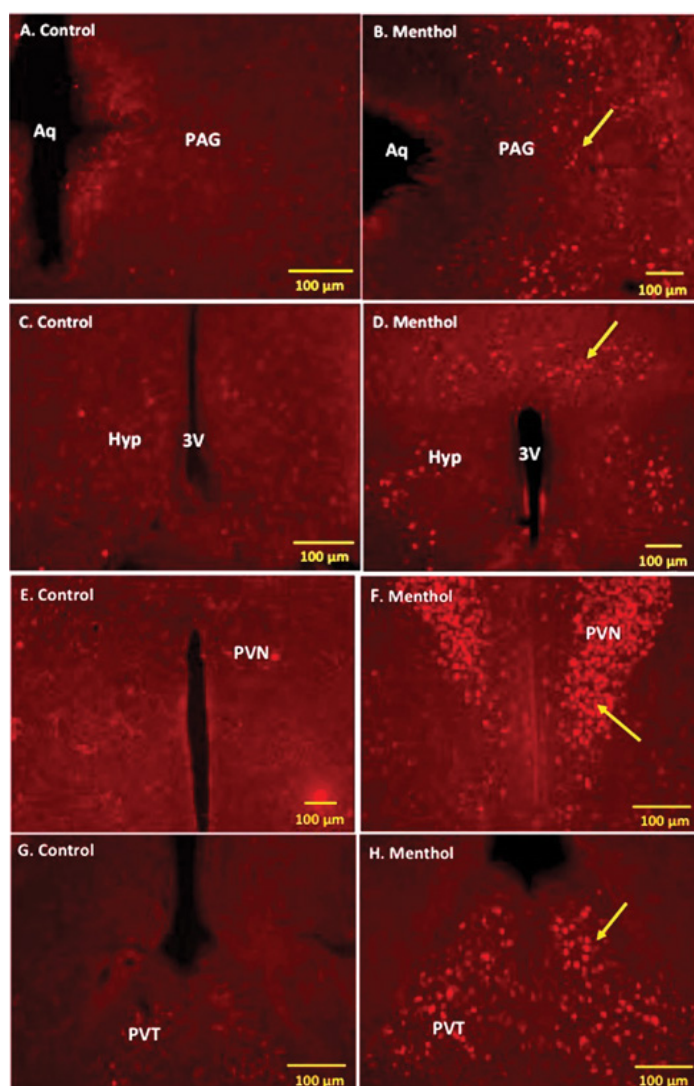


Figure 2: Immunofluorescence staining demonstrating representative menthol-induced c-Fos activated regions of the CNS following intraperitoneal (IP) injection of menthol. Panels A, C, E and G: Representative control data demonstrating c-Fos immunoreactivity observed in periaqueductal gray (PAG), Hypothalamus (Hyp), paraventricular nucleus of hypothalamus (PVN) and paraventricular thalamic nucleus (PVT) following IP injection of vehicle. Panels B, D, F and H: represents c-Fos immunoreactivity observed in PAG, Hyp, PVN and PVT, respectively. Arrows point to representative c-Fos IR neurons following IP injection of menthol. Abbreviations: Aq: Aqueduct; 3V: third ventricle.

nucleus medial part (AOM) and olfactory bulb (OB)

Colocalization of menthol-induced c-Fos activated cells with tyrosine hydroxylase (TH) (dopaminergic) immunoreactive cells (IR)

Consistent with previous studies, TH-IR dopaminergic cells were seen at multiple sites of the reward-addiction circuitry including PAG, DR, rostral-caudal extension of VTA, and hypothalamus. In DR, a small number of c-Fos IR cells were interspersed with midline TH-IR cells. The majority of menthol-activated cells at these sites were located bilateral to the midline TH-IR cells of DR (Figure 3; Panels A-C). In midbrain, menthol-activated cells were seen medial to the TH-IR cells of VTAR and in areas corresponding to RM, IPR, IF and RLi (Figure 3; Panels D-F). In hypothalamus (Hyp), menthol-activated cells were found either in close proximity to, or intermingled with, TH-IR dopaminergic cells (Figure 3; Panels G-I). Virtually none of the TH-IR dopaminergic cells were activated by IP injection of menthol at these sites.

Colocalization of menthol-induced c-Fos activated cells with GABAergic cells

In VTAR, menthol-induced c-Fos activated cells were seen ventral and medial to the GAD67-GFP positive GABAergic cells that

overlaid the red nucleus parvocellular part (RPC). Menthol activated cells were also seen lateral to the GAD67-GFP positive cells of the substantia nigra reticular part (SNR) and substantia nigra compact part, medial tier (SNCM) (Figure 4). In caudal VTA (VTAC), a sparse number of cells were activated by menthol and none of the GAD67-GFP positive GABAergic cells of interpeduncular nucleus (IPN), SNR or mesencephalic reticular formation (mRt) were activated by menthol at these sites (data not shown). In NAcc, and in areas overlapping MO/A25, GAD67 GFP positive cells intermingled with menthol-induced c-Fos IR cells. However, none of the GAD67-GFP containing GABAergic neurons were targets of menthol at these sites (Figure 4; Panels D though I).

DISCUSSION

The present immunohistochemical data demonstrate that menthol stimulates multiple sites in the CNS including structures previously shown to be activated by nicotine. Menthol-activated cells were seen in several areas of the mesolimbic reward-addiction pathways; however, neither dopaminergic nor GABAergic cells were the initial targets of the IP-administered menthol under our experimental conditions.

In the case of tobacco use and e-cigarettes, menthol is always

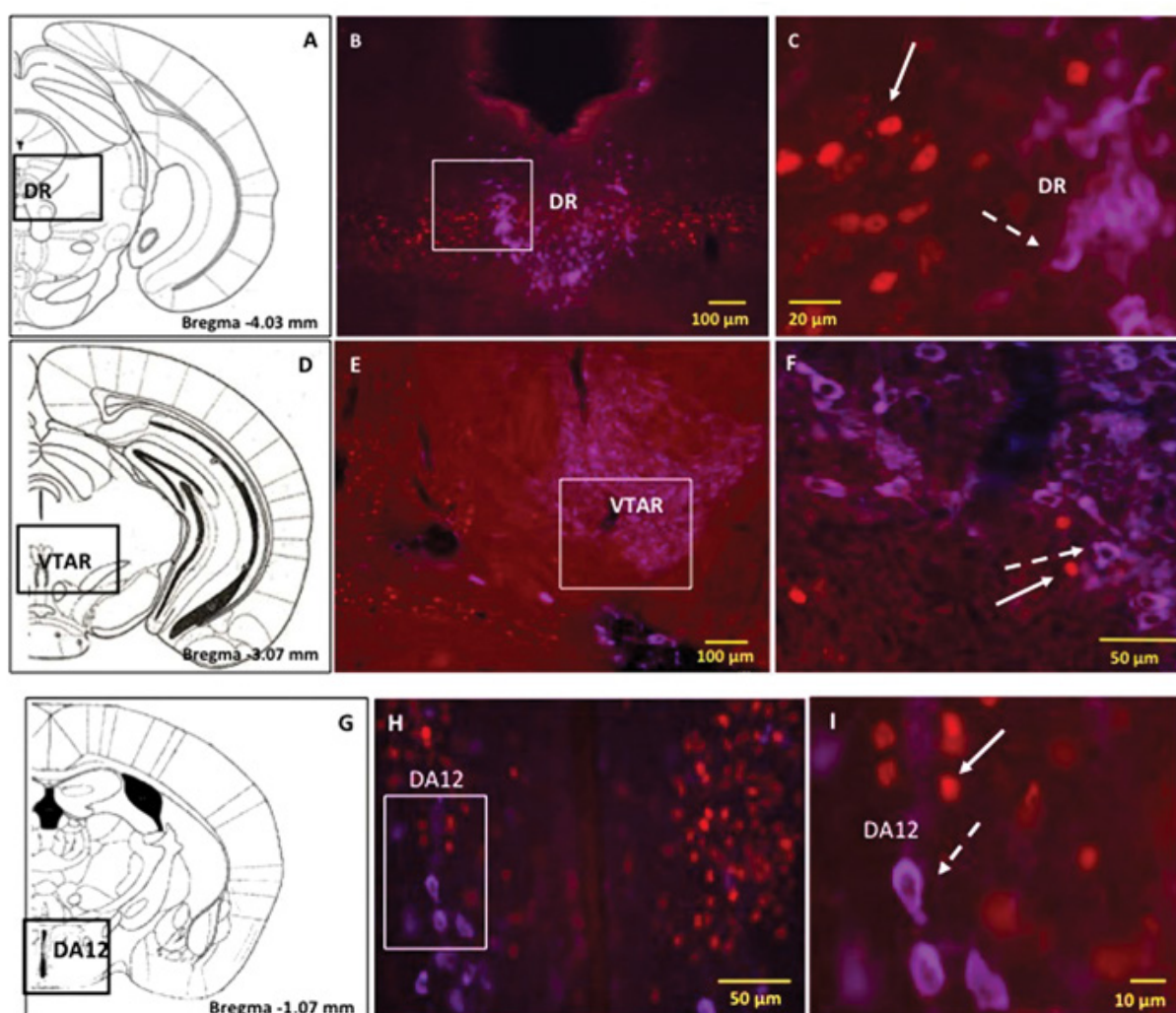


Figure 3: Immunofluorescence staining demonstrating the location of menthol-induced c-Fos activated cells with respect to tyrosine hydroxylase (TH) immunoreactive (IR) dopaminergic cells. Panels A, D and G: Schematic diagrams of coronal sections showing the anatomical location where immunofluorescence merge images of c-Fos and TH-IR dopaminergic cells were captured. Panels B and C; E and F; H and I: Representative low and high power magnification of merged images demonstrating distribution of menthol-induced c-Fos IR cells with respect to TH-IR dopaminergic cells in dorsal raphe (DR), rostral ventral tegmental area (VTAR) and DA12 of hypothalamus, respectively. Solid arrows point to representative c-Fos IR neurons and broken arrows to TH-IR neurons. Squares/rectangles indicate magnified areas. Abbreviations: Aq: Aqueduct; RM: Retromamillary nucleus.

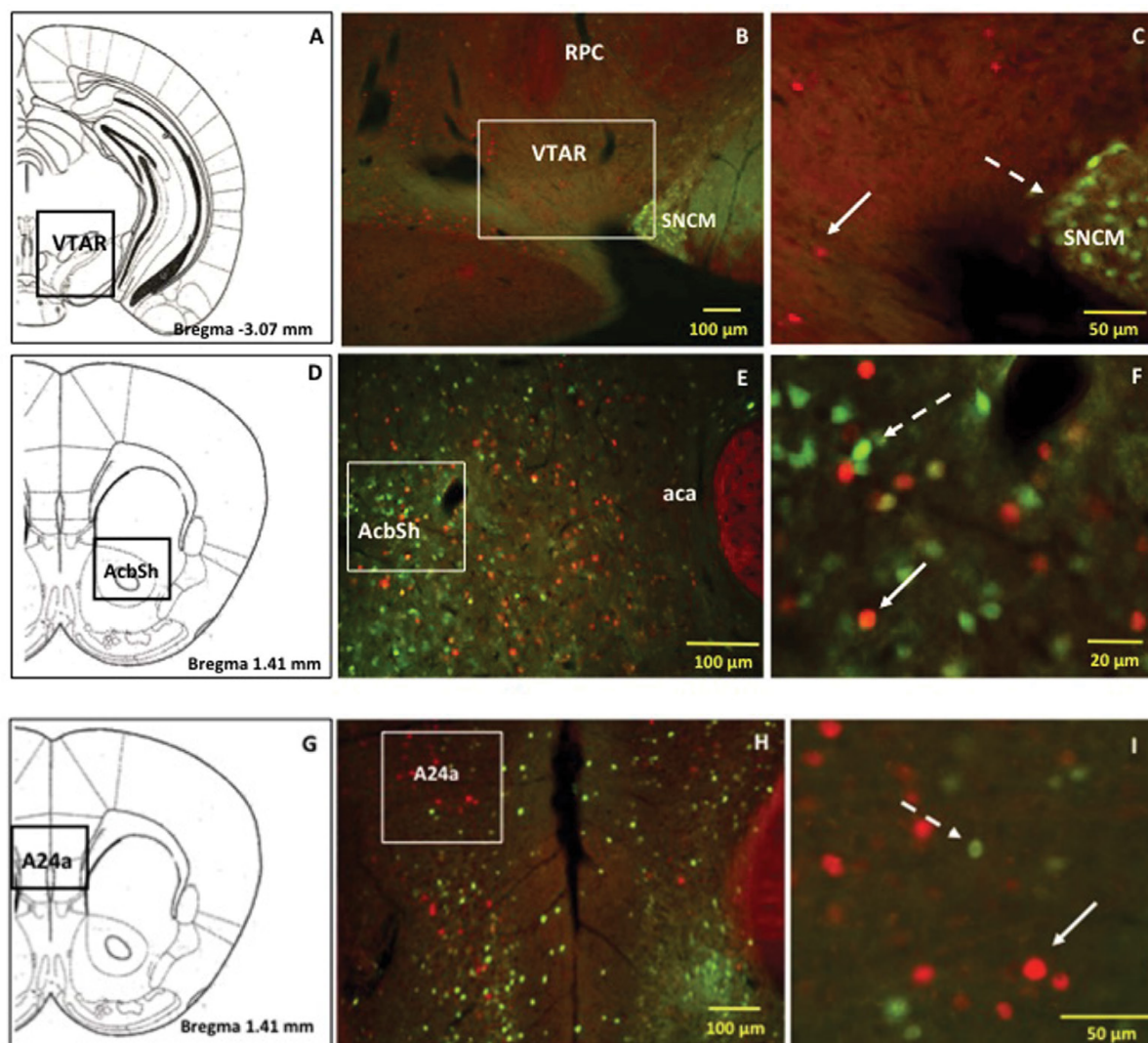


Figure 4: Immunofluorescence staining demonstrating the location of menthol-induced c-Fos activated cells with respect to GAD67-GFP positive cells of the reward-addiction neurocircuitry. Panels A, D and G: Schematic diagrams of coronal sections showing the anatomical location where immunofluorescence image of c-Fos and GAD67-GFP positive cells were obtained. Panels B and C; Panels E and F; Panels H and I: Representative low and high power magnification of merged images demonstrating distribution of menthol-induced c-Fos IR cells with respect to GAD67-GFP positive cells in rostral ventral tegmental area (VTAR), nucleus accumbens (NAcc) and cingulate/orbitofrontal cortex (MO/A25), respectively. Solid arrows point to representative c-Fos IR and broken arrows to GAD67-GFP positive. Squares/rectangles indicate magnified areas. Abbreviations: RPC: Red nucleus, parvocellular part; SNCM: Substantia nigra compact part, medial tier; aca: Anterior commissure, anterior part.

abused in combination with nicotine. However, in the present study we purposefully chose to only look at menthol-induced effects because, combination of menthol and nicotine injection would not have allowed us to distinguish the menthol-induced c-Fos activated cells from nicotine-induced activated cells. Whether the menthol-induced c-Fos activation of CNS neurons observed in the present study is only via menthol stimulation of TRPM8 and TRPA1 receptors on peripheral sensory neurons is not known. Liquid chromatography/tandem mass spectrometric techniques have detected the presence of menthol in the CNS after systemic administration [20]. Intrathecal injection of menthol is reported to induce analgesia [26]. These findings imply that the menthol in cigarette smoke may impact nicotine addiction through both peripheral and central mechanisms. The receptor protein that mediates the direct effects of menthol in the CNS has not been identified. Menthol is shown to serve as a negative allosteric modulator of various nicotinic acetylcholine receptor (nAChR) subtypes [17-19]. Human and animal imaging studies have also shown that menthol causes up-regulation of nAChR binding sites in multiple brain regions [15,16,27]. Thus, nAChRs, which

are densely expressed by neurons in many brain areas, including both VTA and NAcc, are likely targets of menthol in the CNS. Other targets of menthol include kappa opioid receptors (KOR) and GABA_A receptors (GABAAR), which are also expressed at VTA-NAcc sites and are known to mediate the analgesic and antinociceptive properties of menthol [20,28-30]. In situ hybridization and analysis of transgenic expression in reporter mouse strains have confirmed the presence of TRPM8 in the CNS [31], thereby suggesting that TRPM8 may be an additional target of menthol in the CNS.

Both L-menthol [(–)-menthol] and DL-menthol [(±)-menthol] stereoisomers are used in mentholated cigarettes [32]. Previous studies have shown that both (±)-menthol and (–)-menthol upregulated nAChRs, reduced DA neuronal firing frequency and altered DA neuron excitability [15,33]. In the present study using c-Fos to mark cells activated by DL-menthol, we found that dopaminergic neurons were not among the cells initially activated by menthol. Because c-Fos is a marker for cellular activation [24,25, 34,35], we cannot exclude the possibility that menthol may have had an inhibitory effect on the dopaminergic neurons at these

sites. We also found that menthol did not activate the GABAergic neurons in VTA, NAcc, or MO/A25. Since GABA-containing neurons that impact the reward-addiction circuitry may emanate from multiple other sites in the CNS, we cannot rule out the possibility that menthol may have activated GABAergic neurons in brain regions other than those that we studied. Moreover, we identified GABAergic neurons by the expression of green-fluorescent protein in GAD67-containing neurons. The majority of GABAergic neurons in the CNS contain both GAD67 and GAD65 isoenzymes. GAD67-containing GABAergic neurons were not activated by menthol. Since a small proportion of GABAergic neurons may contain GAD65, and not the GAD67 isomer [36-38], it is therefore possible that menthol may have activated GAD65-containing GABAergic neurons, which were not labeled in the present study. Previous reports have shown that menthol increases both phasic and tonic GABAA receptor-mediated currents in midbrain PAG neurons [29]. Menthol-induced enhancement of GABAA receptor-mediated currents has also been shown in spinal cord [20]. Further studies are needed to identify the neurons that are inhibited by menthol activation of GABAAR in the reward-addiction sites.

Many of the CNS areas activated by IP administration of menthol in this study overlap with areas previously reported to be stimulated by topical application of menthol to the skin of mice [39]. These areas are also reported to coincide with the brain regions activated by volatile exposure to menthol [39]. Some of these brain regions are known to be components of the reward-addiction pathways; others may be cortical and subcortical hubs for signaling/integrating information about menthol's cooling, analgesic and flavoring properties. The tobacco industry's choice of menthol as a flavoring agent is, no doubt, related to its minty taste and odor as well as potential effects in reducing the irritation associated with inhaling nicotine. It is well established that gustatory and olfactory sensory perceptions are inextricably linked. Therefore, it is probably not accidental that some cortical and subcortical areas for integrating olfactory signals were, in the present study, sites of neuronal activation by menthol.

CONCLUSION

In summary, the present study identifies multiple areas of the CNS that were activated by acute IP administration of menthol. Dopaminergic and GABAergic neurons of the mesolimbic reward-addiction pathways, however, were not the initial targets of menthol. Our neuroanatomical data corroborate previous behavioural studies suggesting that menthol enhances the addictive properties of nicotine. One of the limitations of this study is that the CNS sites activated by IP administration of menthol may not fully represent the sites stimulated by the inhalation of menthol via smoking mentholated cigarettes or other nicotine delivery devices. Future studies should be designed to determine whether the CNS sites activated by inhalation of menthol are the same as those stimulated by the IP administration.

ACKNOWLEDGMENTS

This work was supported by grants from the Charles and Mary Latham Fund and the Howard University Bridge Fund Pilot Study Awards Program. The authors acknowledge use of the resources provided by the National Institute on Minority Health and Health Disparities of the National Institutes of Health under Award Number G12MD007597. The funding agencies had no role in the study design, collection, analysis or interpretation of the data,

writing the manuscript or the decision to submit the paper for publication.

Declaration of Interests:None declared

REFERENCES

1. Mead EL, Duffy V, Oncken C, Litt MD. E-cigarette palatability in smokers as a function of flavorings, nicotine content and propylthiouracil (PROP) taster phenotype. *Addict Behav.* 2019;91:37-44.
2. Lester JM, Gagosian SY. Finished with Menthol: an evidence-based policy option that will save lives. *J Law Med Ethics.* 2017;45:41-44.
3. Yerger, VB, and McCandless PM. Menthol sensory qualities and smoking topography: a review of tobacco industry documents. *Tob Control.* 2011;20 (Suppl_2): ii37-ii43.
4. Nonnemaker J, Hersey J, Homsy G, Busey A, Allen J, Vallone D, et al. Initiation with menthol cigarettes and youth smoking uptake. *Addiction.* 2013;108:171-178.
5. Muscat JE, Liu HP, Stellman SD, Richie JP. Menthol smoking in relation to time to first cigarette and cotinine: results from a community-based study. *Regul Toxicol Pharmacol.* 2012;63:166-170.
6. Hersey JC, Ng SW, Nonnemaker JM, Mowery P, Thomas KY, Vilsaint MC, et al. Are menthol cigarettes a starter product for youth? *Nicotine Tob Res.* 2006;8:403-413.
7. Levy DT, Blackman K, Tauras J, Chaloupka FJ, Villanti AC, Niaura RS, et al. Quit attempts and quit rates among menthol and non-menthol smokers in the United States. *Am J Public Health.* 2011; 101:1241-1247.
8. Stahre M, Okuyemi KS, Joseph AM, Fu SS. Racial/ethnic differences in menthol cigarette smoking, population quit ratios and utilization of evidence-based tobacco cessation treatments. *Addiction.* 2010; 105:75-83.
9. Gandhi KK, Foulds J, Steinberg MB, Lu SE, Williams JM. Lower quit rates among African American and Latino menthol cigarette smokers at a tobacco treatment clinic. *Int J Clin Pract.* 2009;63:360-367.
10. Gundersen DA, Delnevo CD, Wackowski O. Exploring the relationship between race/ethnicity, menthol smoking, and cessation, in a nationally representative sample of adults. *Prev Med.* 2009;49:553-557.
11. Pletcher MJ, Hulley BJ, Houston T, Kiefe CI, Benowitz N, Sidney S, et al. Menthol cigarettes, smoking cessation, atherosclerosis, and pulmonary function: the Coronary Artery Risk Development in Young Adults (CARDIA) Study. *Arch Intern Med.* 2006;166:1915-1922.
12. Villanti AC, Mowery PD, Delnevo CD, Niaura RS, Abrams DB, Giovino GA, et al. Changes in the prevalence and correlates of menthol cigarette use in the USA, 2004-2014. *Tob Control.* 2016;25:14-20.
13. Corey CG, Ambrose BK, Apelberg BJ, King BA. Flavored tobacco product use among middle and high school students—United States, 2014. *MMWR Morb Mortal Wkly Rep.* 2015;64:1066-1070.
14. Lawrence D, Rose A, Fagan P, Moolchan ET, Gibson JT, Backinger C L, et al. National patterns and correlates of mentholated cigarette use in the United States. *Addiction.* 2010;105:13-31.
15. Henderson BJ, Wall TR, Henley BM, Kim CH, Nichols WA, Moaddel R, et al. Menthol alone upregulates midbrain nAChRs, alters nAChR subtype stoichiometry, alters dopamine neuron firing frequency, and prevents nicotine reward. *J Neurosci.* 2016;36:2957-2974.
16. Alsharari SD, King JR, Nordman JC, Muldoon PP, Jackson A, Zhu AZ, et al. Effects of menthol on nicotine pharmacokinetic, pharmacology and dependence in mice. *PLoS One.* 2015;10:e0137070.
17. Ton HT, Smart AE, Aguilar BL, Olson TT, Kellar KJ, Ahern GP, et al. Menthol enhances the desensitization of human $\alpha 3\beta 4$ nicotinic acetylcholine receptors. *Mol Pharmacol.* 2015;88:256-264.

18. Ashoor A, Nordman JC, Veltri D, Yang KH, Al Kury L, Shuba Y, et al. Menthol binding and inhibition of $\alpha 7$ -nicotinic acetylcholine receptors. *PLoS One*. 2013;8:e67674.
19. Hans M, Wilhelm M, Swandulla D. Menthol suppresses nicotinic acetylcholine receptor functioning in sensory neurons via allosteric modulation. *Chem Senses*. 2012;37:463-469.
20. Pan R, Tian Y, Gao R, Li H, Zhao X, Barrett JE, et al. Central mechanisms of menthol-induced analgesia. *J Pharmacol Exp Ther*. 2012;343:661-672.
21. Ruskin, DN, Anand, R, LaHoste GJ. Menthol and nicotine oppositely modulate body temperature in the rat. *Eur J Pharmacol*. 2007; 559:161-164.
22. Spichiger M, Mühlbauer RC, Brenneisen R. Determination of menthol in plasma and urine of rats and humans by headspace solid phase microextraction and gas chromatography-mass spectrometry. *J Chromatogr B*. 2004;799:111-117.
23. Franklin KB, Paxinos G. The mouse brain in stereotaxic coordinates Academic Press. San Diego. 1997:186.
24. Dehkordi O, Rose JE, Asadi S, Manaye KF, Millis RM, Jayam-Trouth A, et al. Neuroanatomical circuitry mediating the sensory impact of nicotine in the central nervous system. *J Neurosci Res*. 2015;230-243.
25. Dehkordi O, Rose JE, Dávila-García MI, Millis RM, Mirzaei SA, et al. Neuroanatomical relationships between orexin/hypocretin-containing Neurons/Nerve fibers and Nicotine-Induced c-Fos-activated cells of the reward-addiction Neurocircuitry. *J Alcohol Drug Depend*. 2007;5:273. doi:10.4172/2329-6488.1000273.
26. Proudfoot CJ, Garry EM, Cottrell DF, Rosie R, Anderson H, Robertson DC, et al. Analgesia mediated by the TRPM8 cold receptor in chronic neuropathic pain. *Curr Biol*. 2006;16:1591-1605.
27. Brody AL, Mukhin AG, La Charite J, Ta K, Farahi J, Sugar CA, et al. Up-regulation of nicotinic acetylcholine receptors in menthol cigarette smokers. *Int J Neuropsychopharmacol*. 2013;16:957-966.
28. Ugur M, Kaya E, Gozen O, Koylu EO, Kanit L, Keser A, et al. Chronic nicotine-induced changes in gene expression of delta and kappa-opioid receptors and their endogenous ligands in the mesocorticolimbic system of the rat. *Synapse*. 2017;71. Doi: 10.1002/syn.21985.
29. Lau BK, Karim S, Goodchild AK, Vaughan CW, Drew GM. Menthol enhances phasic and tonic GABAA receptor-mediated currents in midbrain periaqueductal grey neurons. *Br J Pharmacol*. 2014;171: 2803-2813.
30. Michaeli A, Yaka R. Dopamine-related drugs act presynaptically to potentiate GABA(A) receptor currents in VTA dopamine neurons. *Neuropharmacology*. 2011;61:234-244.
31. Ordás P, Hernández-Ortego P, Vara H, Fernández-Peña C, Reimúndez A, Morenilla-Palao C, et al. Expression of the cold thermoreceptor TRPM8 in rodent brain thermoregulatory circuits. *J Comp Neurol*. 2019; <https://doi.org/10.1002/cne.24694>
32. Heck JD. A review and assessment of menthol employed as a cigarette flavoring ingredient. *Food Chem Toxicol*. 2010;48:1-38
33. Henderson BJ, Grant S, Chu BW, Shahoei R, Stephanie M. Huard SM, et al. Menthol stereoisomers exhibit different effects on $\alpha 4\beta 2$ nachr upregulation and dopamine neuron spontaneous firing. *ENEURO*. 2018;5(6):0465-18.
34. Douglas RM, Trouth CO, James SD, Sexcius LM, Kc P, Dehkordi O, et al. Decrease CSF pH at ventral brain stem induces widespread c-Fos immunoreactivity in rat brain neurons. *J Appl Physiol* (1985). 2001; 90:475-485.
35. Bullitt E. Expression of c-Fos-like protein as a marker for neuronal activity following noxious stimulation in the rat. *J Comp Neurol*. 1990;296:517-530.
36. Fish KN, Sweet RA, Lewis DA. Differential distribution of proteins regulating GABA synthesis and reuptake in axon boutons of subpopulations of cortical interneurons. *Cereb Cortex*. 2011; 21:2450-2460.
37. Lee HJ, Choi JH, Ahn JH, Lee CH, Yoo KY, Hwang IK, et al. Comparison of GAD65 and 67 immunoreactivity in the lumbar spinal cord between young adult and aged dogs. *Neurochem Res*. 2011; 36:435-442.
38. Esclapez M, Tillakaratne NJ, Kaufman DL, Tobin AJ, Houser CR. Comparative localization of two forms of glutamic acid decarboxylase and their mRNAs in rat brain supports the concept of functional differences between the forms. *J Neurosci*. 1994;14:1834-1855.
39. Beukema P, Cecil KL, Peterson E, Mann VR, Matsushita M, Takashima Y, et al. TrpM8-mediated somatosensation in mouse neocortex. *J Comp Neurol*. 2018;526:1444-1456.